The oxygenic photogranule process for aeration-free wastewater treatment

Ahmed S. Abouhend, Adam Mcnair, Wenye C. Kuo-Dahab, Christopher Watt, Caitlyn S. Butler, Kim Milferstedt, Jérôme Hamelin, Jeongmi Seo, Gitau J. Gikonyo, Khalid. M. El-Moselhy, et al.

The oxygenic photogranule process for aeration-free wastewater treatment

Ahmed S. Abouhend[‡§], Adam McNair[‡], Wenye C. Kuo-Dahab[‡], Christopher Watt[‡], Caitlyn S. Butler[‡], Kim Milferstedt[‖], Jérôme Hamelin[‖], Jeongmi Seo[‡†], Gitau J. Gikonyo[‡], Khalid M. El-Moselhy[§], Chul Park[‡*]

[‡]Department of Civil and Environmental Engineering, University of Massachusetts Amherst, MA 01003, USA.

[§]Marine Pollution Laboratory, National Institute of Oceanography and Fisheries, Hurghada 84511, Egypt.

[‖]LBE, Univ Montpellier, INRA, Narbonne, France.

[†]Department of Environmental Engineering, University of Seoul, Seoul, South Korea.

[*]Corresponding author: chulp@umass.edu

TOC/ABSTRACT ART

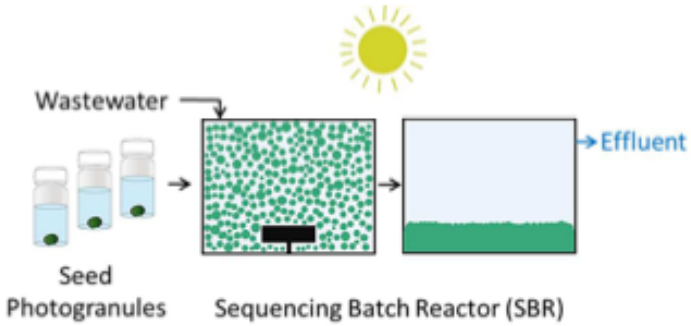

ABSTRACT: This study presents the oxygenic photogranule (OPG) process, a light-driven process for wastewater treatment, developed based on photogranulation of filamentous cyanobacteria, non-phototrophic bacteria, and microalgae. Unlike other biogranular processes requiring airlift or upflow-based mixing, the OPG process was operated in stirred-tank reactors without aeration. Reactors were seeded with hydrostatically-grown photogranules and operated in a sequencing-batch mode for five months to treat wastewater. New reactor biomass propagated with progression of photogranulation under periodic light/dark cycles. Due to effective biomass separation from water, the system was operated with short settling time (10 min) with effective decoupling of hydraulic and solids retention times (0.75 d vs. 21-42 d). During quasi-steady state, the diameter of the OPGs ranged between 0.1 and 4.5 mm. The reactors produced effluents with average total chemical oxygen demand less than 30 mg/L. Nitrogen removal (28-71%) was achieved by bioassimilation and nitrification/denitrification pathways. Oxygen needed for the oxidation of organic matter and nitrification was produced by OPGs at a rate of 12.6±2.4 mg O_2/g biomass-h. The OPG system presents a new biogranule process, which can potentially use simple mixing and natural light to treat wastewater.

INTRODUCTION

Over the past few years, there has been a growing interest in the use of phototrophic granular biomass for wastewater treatment.[1-5] Different from traditional biogranule types, such as aerobic granular sludge (AGS),[6-10] this phototrophic granular biomass contains a significant level of photosynthetic microorganisms. Hence, these phototrophs may autonomously produce O_2 needed for oxidation of organic matter and nitrification, which in the AGS process is often provided by energy-intensive aeration. Similar to the AGS process, the phototrophic granular process allows effective biomass separation from water and enhances the system operation in small footprint.[1,5]

It has been shown that phototrophic granules were produced when different types and sources of biomass were seeded in airlift photobioreactors.[1-4] The seed biomass used includes: 1) activated sludge mixed with microalgal/cyanobacterial biofilm collected from freshwater reservoir;[1] 2) sludge from sedimentation tanks of a wastewater treatment plant (WWTP);[2] 3) AGS mixed with unicellular green algae *Chlorella* and *Scenedesmus*;[3] and 4) mixture of AGS and previously-formed algae-bacterial granules.[4] The use of airlift reactors in these photogranule studies is most likely due to legacy reactor configuration, primarily used for the AGS process and known to provide a pattern of hydraulic shear promoting the formation of biogranules.[6-8,11,12] Another recent paper by Tiron *et al*.[5] reported the formation of phototrophic granules in a stirred-tank photobioreactor; however, the detailed hydraulic characteristics in the reactor were not provided. The seed in this study was also undefined biofilm of activated sludge and algae developed on the inner wall of lab photobioreactors.[5] It can be seen that seeds used in most of photogranule studies are not well-defined due to the lack of some basic information, including

the preparation and characteristics of the seed, which makes it rather difficult to reproduce the start-up of the photogranule process.

We recently reported that phototrophic granules can also be generated by substantially different means[13,14]. Based on Park and Dolan[13] and Milferstedt *et al.*[14] activated sludge transforms into photogranules when incubated under hydrostatic batch conditions with a source of light. Transformation of activated sludge into a photogranule occurred with the enrichment of indigenous motile filamentous cyanobacteria and green algae, which leads to the development of interwoven phototrophic mat, enclosing other microorganisms in a spherical structure.[14] Milferstedt *et al.*[14] also showed that photogranulation is a common phenomenon because photogranules were developed from activated sludge of various sources in different continents. When these hydrostatically-formed photogranules are seeded into reactors for wastewater treatment, offspring photogranules are generated in completely mixed environments.[13,14] Until now, however, no details of seeding, operation and performance of this photogranule reactor have been reported.

Here, we present the oxygenic photogranule (OPG) process, which occurs in stirred-tank reactors seeded with hydrostatically-grown photogranules and operated without aeration. We show the progressive structural development of photogranules from seeding to quasi-steady state operation as well as overcoming the challenges associated with the decreased photogranulation over some periods. The study also reports the basic performance of the OPG system, including the removal of COD, nitrogen, phosphorus, and the settleability of biomass. Finally, we show and discuss the specific oxygen production rate of OPG biomass and how this autonomous oxygen production is related to the mechanism of the OPG process.

MATERIALS AND METHODS

Seed photogranules. The seed photogranules were generated from activated sludge under hydrostatic batch conditions following the procedure shown in Milferstedt *et al.*[14] The detailed steps of the seed formation for the current study are also described in Supporting Information.

Reactor setup and operation. Sixty-one hydrostatically-formed photogranules were seeded into a glass batch reactor containing 1.2 L of primary effluent collected from a local WWTP (Amherst, MA). Mixing at approximately 100 rpm was provided by an overhead stirrer equipped with a stainless-steel impeller of 5 cm in diameter. Light conditions at a photosynthetically active radiation (PAR) of approximately 150 $\mu mol/m^2$-s on the reactor surface were provided by fluorescent-light bulbs. The batch reactor volume was doubled over three days and then split into two 1.2 L reactors that were operated as sequencing-batch reactors (SBRs). After nine days of SBR operation, the reactor volume was increased to the final volume of 1.5 L.

The two SBRs were operated in four 6 h cycles per day at a hydraulic retention time (HRT) of 0.9 d. Each cycle started with a dark phase for 2.5 h, followed by a light phase for 3.5 h. The reactors were operated inside a dark box. During the light phase, each reactor received PAR of approximately 150 $\mu mol/m^2$-s. At the beginning of each cycle, the reactors were fed wastewater over 10 min with mixing. At the end of a cycle, mixing was discontinued and biomass was allowed to settle for 10 min, followed by 2 min effluent decanting.

The two SBRs were operated in the above-mentioned scheme for 46 days. On day 47, HRT was decreased from 0.9 d to 0.75 d. Between days 64 and 72, a short trial was conducted to test the response (COD and N removals) of the reactors to a lower HRT at 0.5 d. On day 73, HRT was returned to 0.75 d until the end of operation. The dark/light sequence in Reactor 1 was

reversed on day 78 to investigate the performance of the system under a different light sequence. We also reduced the light intensity by decreasing PAR from 150 to 100 μmol/m^2-s on days 93 and 81 for Reactors 1 and 2, respectively, to suppress the growth of filamentous green algae.

Hydraulic characteristics of reactors. The average velocity gradient (G) and the Kolmogorov microscale (η) were determined following the procedure shown in Wan *et al.*[15] The determined G and η values were approximately 40 1/s and 160 μm, respectively.

Influent wastewater. We used primary effluent of Amherst WWTP as influent to the OPG systems. Total COD (tCOD) was in the range of 90-300 mg/L with an average of 156±53 mg/L. Total dissolved nitrogen (TDN) ranged between 23 and 49 mg N/L with an average of 33±8 mg/L. Ammonia concentration was 24±7 mg N/L, representing 74±10% of TDN. The remaining portion of TDN was in the form of organic nitrogen. Phosphate was found on average 3.4±0.7 mg P/L. pH ranged between 7.1 and 7.8.

Microscopy. White light and fluorescence microscopy (EVOS FL, AMEFC4300) were used to study progression of photogranulation. Cyanobacteria and green algae were identified using microscopy based on Wehr *et al.*[16]

Imaging and particle size distribution (PSD) analysis. Images of mixed OPG biomass in Petri dishes (5 cm in diameter) were regularly collected and analyzed for PSD using the software ImageJ.[17] The detailed procedure for biomass imaging and PSD analysis are described in Supporting Information.

Oxygen production rate (OPR) of the OPG biomass. Two batch experiments were conducted to determine the OPR of the OPG biomass in the absence and presence of ambient air diffusion. The first batch was conducted in a closed 300 mL BOD bottle filled with mixed OPG biomass with no headspace. The second batch was conducted in an open-top 2 L glass vessel containing 1.5 L of mixed OPG biomass. For both batch experiments, the mixed OPG biomass was collected from SBRs immediately after influent feeding to maintain organic and nitrogen loading conditions similar to those in SBR at the beginning of cycle. The two batches were purged with nitrogen to remove dissolved oxygen (DO). Then, the biomass was mixed using either a magnetic stirrer (closed batch) or overhead stirrer (open batch) and exposed to light at PAR of approximately 150 $\mu mol/m^2$-s. The increase in DO over time was monitored using a BOD probe in the closed system and a regular DO probe in the open system. We ran the closed batch experiment for 1 h because DO got quickly saturated. The open experiment was operated for 6 h. The DO data of the two batch experiments were plotted and "the net OPR (OPR_{net})" of OPG biomass was determined as the slope of the linear-regression line of DO concentrations versus time.

Next, we estimated "the oxygen consumption rate (i.e., $OPR_{consumed}$)" for organic matter oxidation and nitrification in the two batch experiments by tracking the concentrations of COD and nitrogen species in the bulk liquid over time. This analysis required two assumptions: 1) all removal of COD is via aerobic oxidation and 2) only the increase in nitrate-N accounts for nitrification as not all decreases in ammonia-N can be attributed to ammonia oxidation. Then, using the stoichiometric ratio for COD and ammonia to O_2 (1 mg O_2/mg COD and 4.6 mg O_2/mg NH_4^+-N), we determined $OPR_{consumed}$.

The total OPR (OPR_{total}) of the OPG biomass was, therefore, obtained based on the following equation:

$$OPR_{total} = OPR_{net} + OPR_{consumed} \qquad \text{(Eq. 1)}$$

where OPR_{total} is the total OPR of OPG biomass, OPR_{net} is the net OPR of OPG biomass, which was obtained by direct measurements of DO in bulk liquid, and $OPR_{consumed}$ is the theoretical oxygen consumption rate, which was determined based on the equivalent amounts of oxygen consumed for organic matter oxidation and nitrification over time.

The specific OPR (SOPR) of OPG biomass was then determined using the following equation:

$$SOPR = OPR_{total} / X_{OPG} \qquad \text{(Eq. 2)}$$

where OPR_{total} is the total OPR of OPG biomass and X_{OPG} is the biomass concentration in the system.

We also ran controls to both closed and open batch experiments. For the closed batch, three types of controls free of organic matter were run. The OPG biomass was separated from bulk liquid and resuspended in deionized water, tap water, and modified synthetic growth medium [Na_2HPO_4 (1.4 mg/L), KH_2PO_4 (0.9 mg/L), $MgSO_4$ (0.05 mg/L), $CaCl_2$ (0.04 mg/L), and trace metal mix (1 mL/L)]. For open batch, a control was run without the OPG biomass to determine the oxygen transfer rate (OTR) due to mixing in an open batch. The increase in DO due to air diffusion into bulk liquid was monitored until the saturation point. Then the volumetric oxygen mass transfer coefficient (K_La) was determined as the slope of $\ln(C_{sat} - C_L)$ versus time.[18] The OTR was determined for the first 1 h, 1-3 h, and the last 3-6 h in open batch using this equation: $OTR = K_La\ (C_{sat} - C_L)$.[18] The obtained OTR was deducted from OPR_{total} obtained from open batch sets. All batch experiments and controls were done in triplicate.

Biomass yield. The observed yield of OPG biomass (Y_{obs}) is presented as g VSS produced/g tCOD consumed or g tCOD produced/g tCOD consumed. To determine the Y_{obs} of each reactor, we used a liner-regression analysis method shown in Chon *et al.*[19]

Analytical methods. Total and volatile suspended solids (TSS and VSS) and chlorophyll *a* of OPG biomass were determined following Standard Methods[20] 2540D/E and 10200H, respectively. Total and soluble COD of samples were also determined according to Standard Methods (5220D).[20] Soluble fractions were obtained by filtering samples using 0.45 μm filters. These soluble samples were used for determining TDN, measured by TOC/TN analyzer (TOC-VCPH, Shimadzu). We determined the concentrations of ammonia in influents and effluents using the semi-automated colorimetry method.[21] Nitrate and nitrite were measured using ion chromatography (Metrohm 830). Sludge volume index (SVI) and settling velocity were determined following Standard Methods (2710D/E).[20] The settling velocity of individual granules was measured in a graded glass cylinder containing reactor effluent. DO and pH of the samples were measured using a portable DO meter (Extech 407510A) and a bench-top pH meter (Corning 320).

Statistics. Data were graphed using *MS Excel 2013*. We used the unpaired t test to examine the statistical significance between the results.

RESULTS AND DISCUSSION

Reactor seeding and protogranule formation in batch operation. We seeded hydrostatically-formed photogranules in a reactor containing wastewater and operated it in batch for four days. Unlike AGS and other phototrophic granule systems requiring airlift reactors[1-8,11,12], our photogranule systems were not aerated and mixing of biomass was provided from overhead stirring with an impeller.

Over the first day of batch operation, seed photogranules started breaking up, releasing many 100-200 μm aggregates into bulk liquid (Figure 1a-b). These aggregates were not spherical but possessed motile filamentous cyanobacteria as well as unicellular green algae and bacterial biomass. Based on microscopic observation and the morphological information provided in Wehr *et al.*,[16] the filamentous cyanobacteria in these aggregates belong to members of the order *Oscillatoriales* (putatively, *Oscillatoria* sp. and *Microcoleus* sp.) while the unicellular green algae belong to members of the family *Scenedesmaceae* (predominantly, *Acutodesmus* sp. and *Scenedesmus* sp.). Based on DNA sequencing analysis, Milferstedt *et al.*[14] also showed that *Microcoleus* and *Acutodesmus* are the most abundant phototrophs in both hydrostatically-formed photogranules and photogranules generated in flow-based reactors.

Over the remaining batch period, the biomass size progressively increased with more spherical shape appearing, which seemed to happen with continuous growth of filamentous cyanobacteria in the biomass (Figure 1c-e). On day 4, the size of biomass was in the range of 90-600 μm with an average of 250±90 μm, suggesting a granular system. The number of discernible biomass particles also greatly increased over the batch period, from 61 seed granules to about 435,000±199,000 aggregates/granules (Figure S1).

Disintegration of seed photogranules and the formation of numerous new photogranules during this period is very likely enhanced by hydrodynamic shear caused by mixing. It has been

shown in many studies that shear stress is required for granule formation.[7,12,22-24] However, shear alone cannot account for the photogranulation phenomenon, because otherwise photogranules in hydrostatic cultivation should not have been formed in the absence of shear. Nonetheless, shear likely plays an important role in flow-based operation of the OPG systems, including start-up, and may influence granule structure and characteristics. It has also been reported in the literature that relatively high hydrodynamic shear force can lead to the formation of more compact and denser granules than the system with low shear stress.[7,22,25,26]

Size evolution of OPG biomass in SBRs. Figure 2 shows the evolution of PSD in SBRs over a five-month period. Over the first 50 days, the size of photogranules gradually increased with a range of 0.1-1.5 mm and an average diameter of 0.45±0.2 mm. By day 50, biomass less than 250 μm represented the highest number of biomass in SBRs (Figure 2a). However, the mean size of biomass in terms of biovolume already reached about 0.75 mm (Figure 2b). During the remaining operation period, PSD becomes wider and shifts towards larger-size particles. On day 106 and 150, the peaks in PSD were observed at OPG diameters of 1.7 and 2.9 mm, respectively (Figure 2b). During this period, the number of photogranules smaller than 1 mm was still dominant. However, the majority of biovolume was caused by photogranules greater than 1 mm. Towards the end of reactor operation, more than 90% of total biovolume in SBRs was caused by photogranules larger than 1 mm (Figure 2b).

The largest size of OPGs in reactors was approximately 4.5 mm and continuous operation did not lead to further increase in granule size. This value is much greater than the size of photogranules (≤ 2 mm in diameter) reported from the previous photogranule reactor studies.[2-5] For AGS, the largest granule size has been in the range of 4-6 mm.[7,27] We also observed that the

total number of photogranules in the systems was not constant (Figure S1), likely due to several factors, including changes in the strength of wastewater and biomass wasting schemes, which are discussed later in this study.

Changes in morphology of photogranule biomass in SBRs. During the first two months of SBR operation, granules became bigger and more spherical (Figure 3a-d). Between days 70 and 90, there was overgrowth of filamentous green algae, predominantly *Stigeoclonium* sp. (Figure 3e). Based on microscopy, these filamentous green algae were not entrenched in the granules but mostly grew either on the surface of photogranules or freely in bulk liquid. Our preliminary studies showed that lower illumination levels can enhance the growth of filamentous cyanobacteria over filamentous green algae. Thus, we decreased the light intensity (PAR 150 to 100 $\mu mol/m^2$-s) on days 93 and 81 for Reactors 1 and 2, respectively. This change brought a positive impact on reactor operation by promoting cyanobacteria-based granulation (Figure 3f-h). Different from *Oscillatoria* and *Microcoleus*, which are motile, non-branched filamentous cyanobacteria, *Stigeoclonium* are non-motile but branched filamentous green algae.[16] Deterioration of photogranulation by excessive growth of *Stigeoclonium*, therefore, suggests that not all filamentous phototrophs but a group with non-branching and motility characteristics can lead to photogranulation.

Biomass concentration and settleability. Biomass concentrations increased as the number and size of the biomass increased during SBR operation. For the first two weeks, TSS increased from approximately 900 to 2,300 mg/L (Figure S2). Over this period, reactors were maintained with no biomass wastage except for sampling. On day 19, we started regular biomass wastage. The

volume of daily biomass wastage ranged between 30-90 mL of mixed biomass. In addition, there were a couple of big wasting events by removing $1/6^{th}$ to $1/3^{rd}$ of settled biomass during early operation period (days 35-70) when the system became quite crowded (TSS > 3,000 mg/L). Based on this wastage scheme, the monthly solids retention times (SRTs) of the systems remained between 21 and 42 d with an average of 32 d. During the remaining operation period, the average biomass concentration in reactors remained at 2,750±620 mg/L with a volatile fraction at 86±3%.

Effective biomass separation through the production of fast-settling biomass is one main advantage of biogranular processes. During the first two months, SVI of photogranule biomass decreased from its initial value of 103 to 61 mL/g, indicating progression of granulation (Figure S3). During the same period, ZSV of mixed OPG biomass increased from an average of 3.2 to 9.6 m/h (Figure S3). The overgrowth of filamentous green algae during days 70 and 90 (Figure 3e-f) resulted in decrease in biomass settleability. Controlling the growth of filamentous green algae with the reduced light intensity improved biomass settleability. Towards the end of reactor operation, the mixed OPG biomass showed SVI of 53±2 mL/g and ZSV of 14.6±0.5 m/h. These values indicate substantially better biomass settling characteristics than the field activated sludge. The activated sludge from the WWTP where we collected wastewater to feed the current OPG systems showed SVI in 300-400 mL/g and ZSV in 0.1-0.2 m/h.

The individual photogranules of 1-4.5 mm in diameter showed the settling velocities in the range of 26-91 m/h, higher than the settling velocities reported for AGS (10-40 m/h).[8,28-32] Density and porosity of OPGs at various sizes can potentially reveal more information about the physical properties of OPGs but they were beyond the scope of the current study. The efficiency

of the OPG biomass separation with respect to the removal of TSS and chlorophyll *a* after 10 min settling were both greater than 99%.

COD removal. The organic loading rate (OLR) in reactors varied due to changes in the strength of influent and HRT of the OPG system. During the entire operation period, the OLR fluctuated between 106 and 405 mg COD/L-d (Figure 4). Over the first 46 days (0.9 d HRT), the average OLR was 210±84 mg COD/L-d. The removal efficiency and removal rate of tCOD during this period were 77±9% and 223±111 mg COD/d, respectively.

The decrease in wastewater strength at the WWTP after day 46 motivated us to operate the SBRs at shorter HRTs. On day 47, we reduced the HRT from 0.9 to 0.75 d for 17 days. During this period, the OLR was 170±37 mg COD/L-d, which was still lower than that of the earlier period. The tCOD removal efficiency during this period increased to 86±4% while the tCOD removal rate remained at 230±52 mg COD/d. We again reduced HRT to 0.5 d on day 64 to test the response (COD and N removals) of the reactors to a lower HRT. Due to the reduced HRT as well as high influent strength observed during this period, the OLR significantly increased to an average of 312±53 mg COD/L-d. The tCOD removal efficiency during this period did not change noticeably (82±3%) while the tCOD removal rate substantially increased (432±78 mg COD/d). After nine days at 0.5 d HRT, we increased the HRT back to 0.75 d and kept it the same until the end of operation. During the remaining 76 days of operation, the average OLR, tCOD removal efficiency, and tCOD removal rate were 190±37 mg COD/L-d, 78±5%, and 239±56 mg COD/d, respectively. Although the light sequence in Reactor 1 was reversed on day 78, effluent COD of the two reactors remained very similar until the end of

operation. Also, the tCOD removal rates of the two SBRs during this period were nearly identical; 235±55 and 236±57 mg COD/d for Reactor 1 and 2, respectively.

Despite significant variation in OLR during five-month period, the average effluent tCOD in both SBRs was less than 30 mg/L (Figure 4), meeting typical requirements for municipal wastewater treatment in developed countries. A similar COD removal efficiency can be achieved in AGS systems with energy-intensive aeration.[6-8,29,33]

Nitrogen removal. Nitrogen loading rate (NLR) in SBRs also varied with changes in influent and HRT. NLR ranged between 30 and 98 mg N/L-d with an average of 43±13 mg N/L-d, while ammonia loading rate (ALR) was in the range of 19-57 mg N/L-d with an average of 31±9 mg N/L-d (Figure 5a-b).

In contrast to COD, N removal in OPG systems was sensitive to NLR as well as OLR (Figure 4; Figure 5a-b; Figure S4). The first stable NH_4^+ removal was achieved after approximately three weeks of operation. Removal of ammonia was accompanied with some level of nitrite and nitrate appearing in effluents, suggesting the occurrence of active nitrification (Figure S4). After about a month of operation, ammonia removal efficiency reached 90-96% with high level of nitrate in effluents, indicating that stable nitrification was established in the OPG systems. TDN removal also reached 57 and 52 % in Reactor 1 and Reactor 2, respectively, after about a month of operation. Over the first two months of operation, where the two SBRs were operated under the same operating conditions (i.e., duplicate), TN removal profiles of the two reactors were quite similar.

A sudden increase in OLR as well as NLR and ALR, which started on day 61, resulted in substantial loss of nitrification (Figure 5a-b; Figure S4). Similar to NH_4^+ removal, TDN removal

also substantially decreased during the same period; positive correlations were found between effluent TDN and NH_4^+ in both reactors (R^2 = 0.68 and 0.75 in Reactor 1 and 2, respectively). These results, therefore, suggest that nitrification/denitrification is an important pathway for nitrogen removal in the studied OPG systems. The evidence of nitrification and denitrification in OPG systems can also be supported by molecular ecology information. Earlier, Milferstedt *et al.*[14] reported the presence of nitrifiers in the reactor photogranules at the same level as hydrostatic photogranules and the activated sludge inocula from which hydrostatic photogranules were generated. Furthermore, Stauch-White *et al.*[34] showed the presence of nitrification and denitrification genes, *amoA* and *narG*, respectively, in the seed photogranules.

It is worth noting that effective COD removal continued to occur although nitrification was inhibited (Figures 4 and 5). It is very likely that when OLR and NLR increase, nitrifying bacteria are outcompeted by heterotrophic bacteria for the limited amount of O_2 because nitrifiers are much more sensitive to O_2 level than heterotrophs.[35] Nitrification and TDN removal started to recover when NLR and OLR started decreasing after day 73 (Figure 5a-b; Figure S4).

After reversing the light sequence in Reactor 1 on day 78 from Dark→Light to Light→Dark, the two reactors started showing different TDN removal (Figure 5a). Over the last two months of operation, the TDN removal efficiency was 41±7% in Reactor 1 vs. 55±8% in Reactor 2, which is a significant difference (p-value<0.01). This implies that pre-dark conditions available in Reactor 2, so in this reactor a cycle starts with feed in the absence of oxygen but with nitrate, promotes additional nitrogen removal by denitrification in the OPG process, similar to pre-anoxic or pre-denitrification processes for biological nitrogen removal.[35]

Phosphorus removal. The loading rate of PO_4^{3-} in SBRs was in the range of 3.1-9.2 mg P/L-d (Figure 5c). Phosphate was removed at an average removal efficiency of 21±11%. The highest PO_4^{3-} removal efficiency of 38-44% was observed between days 60 and 80 along with a significant increase in PO_4^{3-} loading rate and OLR. During this period, high TDN and NH_4^+ were also found in the effluent (27±7 mg N/L and 17±7 mg N/L, respectively) due to the loss of nitrification. These high levels of organic matter and nutrients in reactors resulted in a substantial increase in OPG biomass which allowed us to operate the SBRs at SRT of 18 d, which was about two times shorter than SRTs of the earlier and later periods of operation. Removal of phosphorous by chemical precipitation did not likely occur in our OPG reactors as the pH of bulk liquid never exceeded 7.5.

Production of O_2 by OPGs. Figure 6a presents the determined SOPR of OPG biomass in a closed batch system (thus, no interaction with ambient air) containing wastewater or three control waters devoid of organic matter. The SOPR of OPG biomass in wastewater was 12.6±2.4 mg O_2/g VSS-h, much greater than SOPR obtained from the control runs (<1.5 mg O_2/g VSS-h). The high SOPR of OPG biomass in wastewater indicates high functional utility of OPG biomass in wastewater. Very low SOPRs observed in the control runs devoid of organic matter as well as free CO_2 from air indicates minimal photosynthetic activity due to the lack of a carbon source. SOPR values associated with the controls were likely due to either presence of some HCO_3^- in the liquid phase (especially for tap water) or the use of OPG biomass itself as a carbon source. Consequently, substantial differences of SOPRs between the experimental and control sets suggest a symbiotic loop in a closed OPG system where CO_2 utilized by phototrophs to produce O_2 mainly comes from organic matter oxidation by heterotrophs.

Figure 6b presents SOPRs of OPG biomass in an open batch system. The SOPRs of OPG biomass for the three periods, first 1 h, 1-3 h period, and 3-6 h period, were determined to be 11.9±2, 2.1±0.3 and 1.7±0.3 mg O_2/g VSS-h, respectively. The decreasing SOPR of the OPG biomass along with decreasing COD concentration over time (53±3, 26±1 and 17±1 mg COD/L at t=0 h, 1h and 3h, respectively) confirms the importance of organic matter as a carbon source in OPG systems. The SOPR value determined for the first one hour in open batch was very similar to the SOPR obtained from the closed batch. The difference may be due to net gas transfer of O_2 by diffusion from the open reactor into the atmosphere.

The K_La and OTR due to mixing in open batch (via control) was determined to be 0.9±0.1 L/h and 35±3 mg O_2/L-d, respectively. Based on OTR, the daily input of atmospheric oxygen into SBRs, which was obtained by multiplying the OTR by the reactor volume (1.5 L), was 53±5 mg O_2/d. On the other hand, the average daily removal of COD and ammonia-N that occurred in the current OPG systems was 254±93 mg COD and 37±11 mg N, respectively, equivalent to about 424 mg O_2/day. This value is eight times higher than that of oxygen transferred from the ambient air via mixing, suggesting that oxygen demand in the OPG SBR was primarily satisfied by internal O_2 production by OPG biomass. The obtained SOPR of OPG biomass can be used as a key design parameter for future OPG reactor studies while a similar concept will be employed for CO_2 balance within the system in the future.

Biomass yield. We determined the growth yield of the OPG biomass using a linear-regression analysis on the amounts of biomass produced per the amounts of influent tCOD consumed. We consider this approach reasonable, because the results of oxygen production experiments shown above indicate that COD is the primary carbon source for the OPG system.

Based on this approach, the yield analysis for the entire operation period showed 0.70 and 0.62 g VSS/g tCOD for Reactors 1 and 2, respectively (Figure S5). The stoichiometric ratio of COD/VSS of the OPG biomass was experimentally determined to be 1.80±0.09. Thus, these observed yields are equivalent to 1.26 and 1.17 g COD/g COD for Reactor 1 and 2, respectively. These values are greater than typical observed yields of activated sludge (0.3-0.5 g COD/g COD),[36,37] which implies phototrophic assimilation of CO_2 into the OPG biomass during SBR operation. These results imply that the OPG process has the potential to recover wastewater's chemical energy (i.e., COD) and solar energy in the form of easily separable granular biomass.

Implications. From seeding to quasi steady-state operation, this study provides a summary of the first successful bench-scale operation of the OPG-based wastewater treatment. The system was operated without uplift mixing and aeration, which are required in many biogranular systems, including recently reported photogranule systems.[1-4] The study also demonstrates effective COD removal and nitrification without aeration due to OPGs' oxygenic photosynthesis. The harnessed symbiotic potential within OPGs resulted in a system with treatment performance satisfying regulatory standards, good settleability for liquid/solid separation and significantly less energy input due to the removal of aeration. Due to photoautotrophic assimilation of CO_2, OPGs also showed biomass yields that are 3-4 times greater than that of activated sludge. This high yield indicates a potential to recover renewable energy in the form of easily-separable biofeedstock, which can be used in downstream processes for energy generation.

Photogranulation of activated sludge under hydrostatic conditions was found to be a universal phenomenon,[14] which implies that any activated sludge can be potentially used to produce seed photogranules. Thus, we expect that seeding the system with hydrostatically-

formed photogranules allows reproducible start-up and operation of the OPG process. Lastly, the OPG system we report here uses stirring-based mixing, different from other photogranule systems, which, we expect, is also important for scale-up and industrialization of the new bioprocess.

ACKNOWLEDGMENTS

This study was supported by National Science Foundation grants (CBET1335816 and CBET1605424) and 2013 Paul Busch Award by Water Environment Research Foundation. ASA was supported by Egyptian Government Scholarship. KM and JH were funded by the French "Agence Nationale de la Recherche" grant (ANR-16-CE04-0001-01).

References:

1. Kumar, R.; Venugopalan, V. P. Development of self-sustaining phototrophic granular biomass for bioremediation applications. *Curr. Sci.* **2015**, *108* (9), 1653-1661.
2. Huang, W.; Li, B.; Zhang, C.; Zhang, Z.; Lei, Z.; Lu, B.; Zhou, B. Effect of algae growth on aerobic granulation and nutrients removal from synthetic wastewater by using sequencing batch reactors. *Bioresour. Technol.* **2015**, *179*, 187-192.
3. Liu, L.; Fan, H.; Liu, Y.; Liu, C.; Huang, X. Development of algae-bacteria granular consortia in photo-sequencing batch reactor. *Bioresour. Technol.* **2017**, *232*, 64-71.
4. Ahmad, J. S. M.; Cai, W.; Zhao, Z.; Zhang, Z.; Shimizu, K.; Lei, Z.; Lee, D.-J. Stability of algal-bacterial granules in continuous-flow reactors to treat varying strength domestic wastewater. *Bioresour. Technol.* **2017**, *244*, 225-233.
5. Tiron, O.; Bumbac, C.; Manea, E.; Stefanescu, M.; Lazar, M. N. Overcoming Microalgae Harvesting Barrier by Activated Algae Granules. *Sci. Rep.* **2017**, *7* (1), 1-11.
6. Morgenroth, E.; Sherden, T.; van Loosdrecht, M. C. M.; Heijnen, J. J.; Wilderer, P. A. Aerobic granular sludge in a sequencing batch reactor. *Water Res.* **1997**, *31* (12), 3191-3194.
7. Beun, J. J.; Hendriks, A.; van Loosdrecht, M. C. M.; Morgenroth, E.; Wilderer, P.A.; Heijnen, J. J. Aerobic granulation in a sequencing batch reactor. *Water Res.* **1999**, *33*, 2283-2290.
8. Beun, J. J.; van Loosdrecht, M. C. M.; Heijnen, J. J. Aerobic granulation in a sequencing batch airlift reactor. *Water Res.* **2002**, *36*, 702-712.
9. Ni, B. J.; Xie, W. M.; Liu, S. G.; Yu, H. Q. Granulation of activated sludge in a pilot-scale sequencing batch reactor for the treatment of low strength municipal wastewater. *Water Res.* **2009**, *43*, 751-761.
10. Gao, D.; Liu, L.; Liang, H.; Wu, W. M. Aerobic granular sludge: characterization, mechanism of granulation and application to wastewater treatment. *Crit. Rev. Biotechnol.* **2011,** *31* (2), 137-152.
11. de Kreuk, M. K.; van Loosdrecht, M. C. M. Formation of aerobic granules with domestic sewage. *J. Environ. Eng.* **2006**, *132* (6)**,** 694-697.

12. Liu, Y.; Wang, Z. W. Selection pressure theory for aerobic granulation in sequencing batch reactors. In *Wastewater purification: aerobic granulation in sequencing batch reactors*; Liu, Y., Eds.; CRC Press: Florida 2007; pp 85-110.

13. Park, C.; Dolan, S. Algal-sludge granule for wastewater treatment and bioenergy feedstock generation. *Patent Cooperation Treaty,* **2015**, WO2015112654 A2.

14. Milferstedt, K.; Kuo-Dahab, W. C.; Butler, C. S.; Hamelin, J.; Abouhend, A. S.; Stauch-White, K.; Mcnair, A.; Watt, C.; Carbajal-González, B. I.; Dolan, S.; Park, C. The importance of filamentous cyanobacteria in the development of oxygenic photogranules. *Sci. Rep.* **2017**, *7* (1), 1-15.

15. Wan, J.; Mozo, I.; Filali, A.; Liné A.; Bessière, Y.; Spérandio, M. Evolution of bioaggregate strength during aerobic granular sludge formation. *Biochem. Eng. J.* **2011**, *58-59*, 69-78.

16. Wehr, J. D., Sheath, R. G, Kociolek, J. P., Eds. *Freshwater Algae of North America: Ecology and Classification*, 2nd, ed.; Academic Press: Cambridge, 2015.

17. Schneider, C. A.; Rasband, W. S.; Eliceiri, K. W. NIH Image to ImageJ: 25 years of image analysis. *Nat. Meth.* **2012**, *9* (7), 671-675.

18. Garcia-Ochoa, F.; Gomez, E. Bioreactor scale-up and oxygen transfer rate in microbial processes: An overview. *Biotechnol. Adv.* **2009**, *27* (2), 153-176.

19. Chon, D. H.; Rome, M.; Kim, Y. M.; Park, K. Y.; Park, C. Investigation of the sludge reduction mechanism in the anaerobic side-stream reactor process using several control biological wastewater treatment processes. *Water Res.* **2011**, *45* (18), 6021-6029.

20. Rice, E.W., Baird, R.B., Eaton, A.D., Clesceri, L. S., Eds. *Standard methods for the examination of water and wastewater*, 22nd, ed.; APHA, AWWA, WEF; USA, 2012.

21. *Method 350.1: Determination of ammonia nitrogen by semiautomated colorimetry*; Revision 2; U.S. Environmental Protection Agency: Cincinnati, OH, 1993.

22. Liu, Y.; Tay, J. H. The essential role of hydrodynamic shear force in the formation of biofilm and granular sludge. *Water Res.* **2002**, *36* (7), 1653–1665.

23. Pan, K.; Su, K.; Zhang, S.; Sun, Z.; Xu, D.; Liu, S. Hydrodynamics and permeability of aerobic granular sludge: The effect of intragranular characteristics and hydraulic conditions. *Biochem. Eng. J.* **2016**, *113*, 133-140.

24. Alphenaar, P. A.; Visser, A.; Lettinga, G. The effect of liquid upward velocity and hydraulic retention time on granulation in UASB reactors treating wastewater with a high sulphate content. *Bioresour. Technol.* **1993**, *43* (3), 249-258.

25. Van Loosdrecht M. C. M.; Eikelboom D.; Gjaltema A.; Mulder A.; Tijhuis L.; Heijnen J. J. Biofilm structures. *Water Sci. Technol.* **1995**, *32* (8), 35-43.

26. Ren, T. T.; Mu, Y.; Liu, L.; Li, X.-Y.; Yu, H. Q. Quantification of the shear stresses in a microbial granular sludge reactor. *Water Res.* **2009**, *43* (18), 4643-4651.

27. Jungles, M. K.; Campos, J. L.; Costa, R. H. R. Sequencing batch reactor operation for treating wastewater with aerobic granular sludge. *Braz. J. Chem. Eng.* **2014**, *31* (1), 27-33.

28. Peng, D.; Bernet, N.; Delgenes, J. P.; Moletta, R. Aerobic granular sludge - a case study. *Water Res*. **1999**, *33*, 890-893.

29. Ni, B. J.; Xie, W. M.; Liu, S. G.; Yu, H. Q. Granulation of activated sludge in a pilot-scale sequencing batch reactor for the treatment of low strength municipal wastewater. *Water Res*. **2009**, *43*, 751-761.

30. Liu, Y.; Yang, S. F.; Tay, J. H. Elemental compositions and characteristics of aerobic granules cultivated at different substrate N/C ratios. *Appl. Microbiol. Biotechnol*. **2003**, *61*, 556-561.

31. Arrojo, B.; Mosquera-Corral, A.; Garrido, J. M.; Mendez, R. Aerobic granulation with industrial wastewater in sequencing batch reactors. *Water Res*. **2004**, *38*, 3389-3399.

32. Zheng, Y. M.; Yu, H. Q.; Sheng, G. P. Physical and chemical characteristics of granular activated sludge from a sequencing batch airlift reactor. *Process Biochem*. **2005**, *40*, 645-650.

33. Su, K. Z.; Yu, H. Q. Formation and characterization of aerobic granules in a sequencing batch reactor treating soybean processing wastewater. *Environ. Sci. Technol*. **2005**, *39* (8), 2818-2827.

34. Stauch-White, K.; Srinivasan, V. N.; Kuo-Dahab, W. C.; Park, C.; Butler, C. S. The role of inorganic nitrogen in successful formation of granular biofilms for wastewater treatment that support cyanobacteria and bacteria. *AMB Express*. **2017**, *7* (1), 1–10.

35. Rittmann, B. E., McCarty, P. L., Eds. *Environmental biotechnology: principles and applications*; McGraw-Hill: New York, 2001.

36. Shi, C. Y. *Mass flow and energy efficiency of municipal wastewater treatment plants*; IWA publishing: London, 2011.

37. Eom, H.; Brennan, A.; Watt, C.; Chon, D.; Park, C. Performance of a pilot, high-rate anaerobic-side-stream process: minimized sludge production and generation of biogas. WEF proceeding. **2013**, Sessions 35-43, 2669-2686.

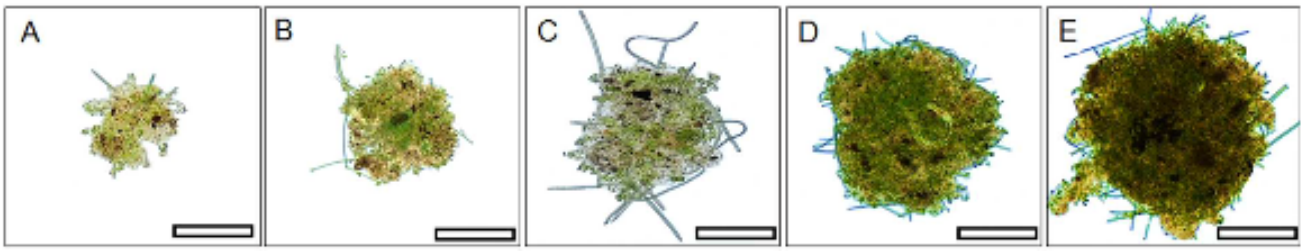

Figure 1. Progression in photogranulation during the reactor startup period (the first four days of batch operation). Biomass from the batch reactor: (A) a few hours after reactor seeding and batch operation, (B) day 1, (C) day 2, (D) day 3, and (E) day 4. The images reveal the enrichment of filamentous cyanobacteria along with increase in the size of biomass and its circularity development. Scale bar for the five panels is 200 µm.

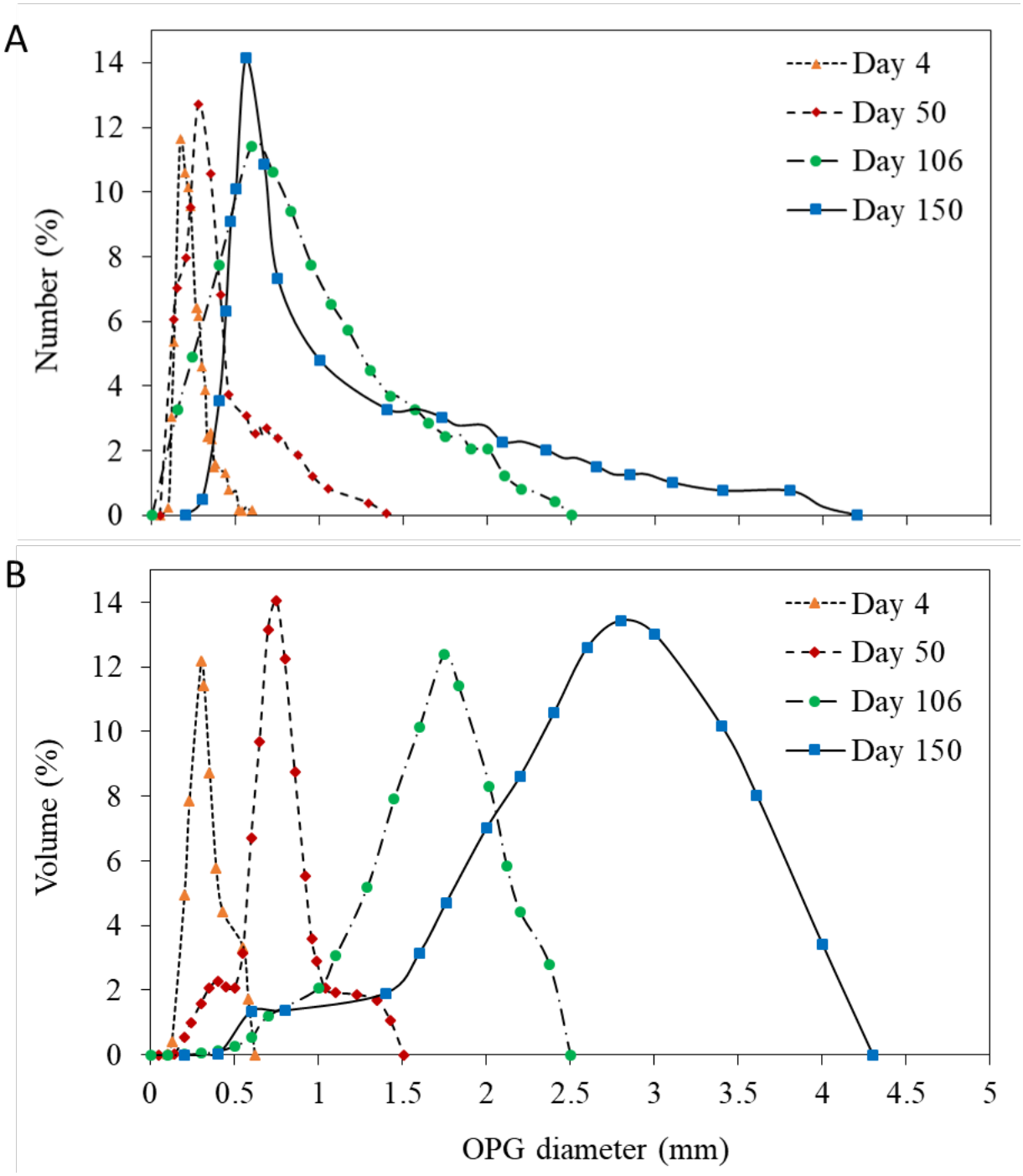

Figure 2. Evolution of particle size distribution (PSD) in reactors over five months of operation. (A) the number-based PSD. (C) the biovolume-based PSD.

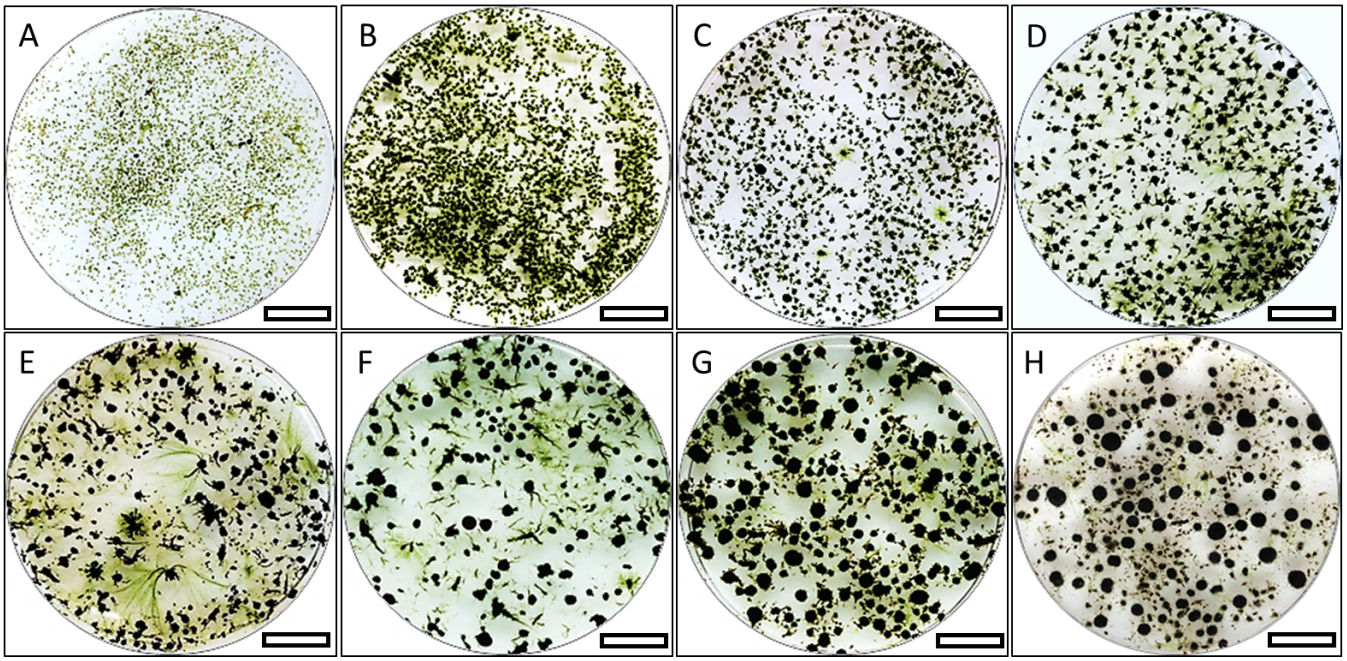

Figure 3. Development of the oxygenic photogranule biomass in reactors over 150 days of operation. Eight petri dish images of the mixed biomass are shown over the batch (the first four days as batch before SBR) and SBR operation periods (day 1-150). (A) day 4 in the batch, (B) day 22, (C) day 50, (D) day 65, (E) day 81, (F) day 96, (G) day 125, and (H) day 150. Scale bar for the eight panels is 1 cm.

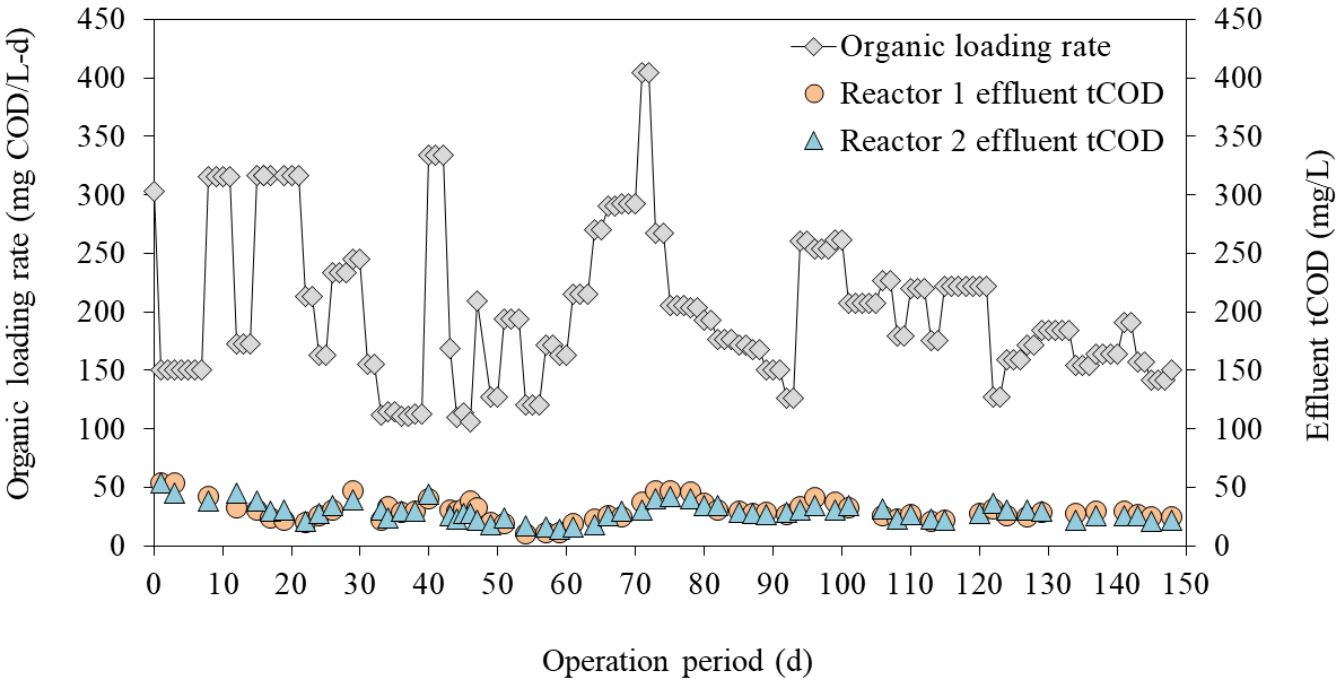

Figure 4. Removal of total COD in reactors over five months of operation along with the changes in the organic loading rate. The organic loading rate (OLR) in reactors varied due to changes in the strength of influent wastewater and HRT of the OPG system. The influent was primary effluent wastewater collected from a local WWTP.

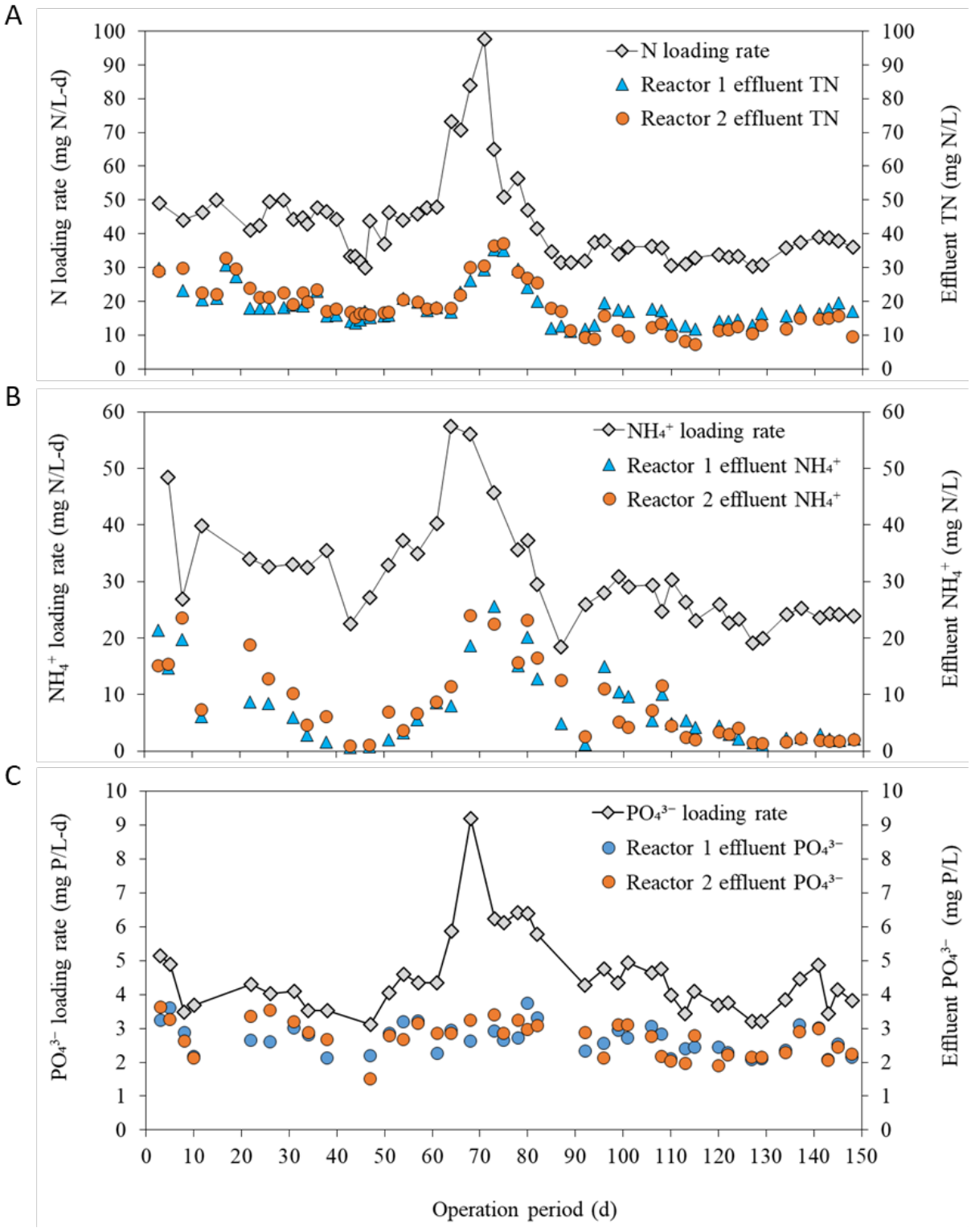

Figure 5. Nutrients removal in OPG systems over five months of operation. Removal of (A) total dissolved nitrogen (TDN), (B) ammonia, and (C) phosphate.

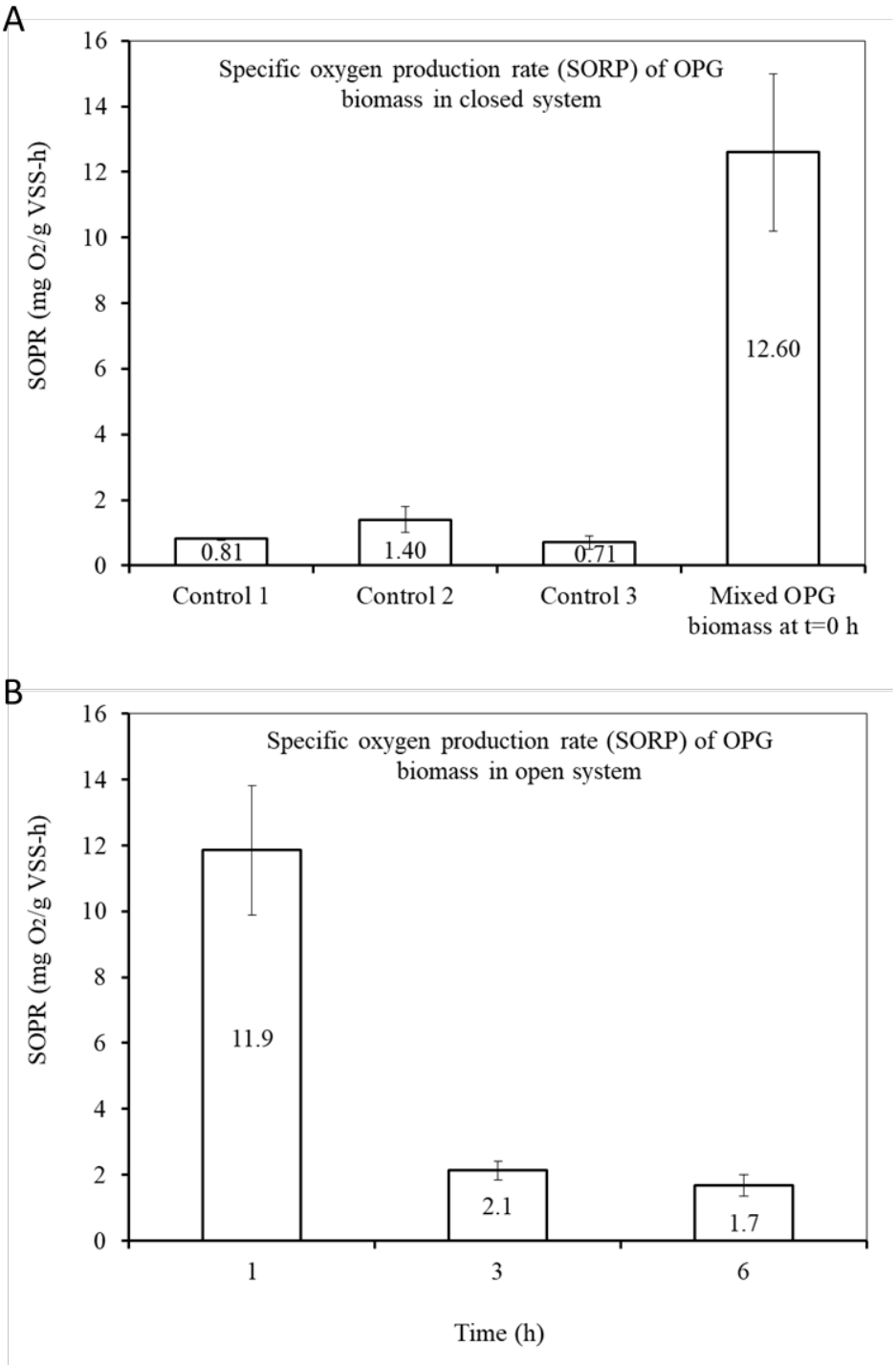

Figure 6. The specific oxygen production rate (SOPR) of mixed OPG biomass determined for closed and open batch systems. (A) Closed system. The three controls for this closed system were run with deionized water (Control 1), tap water (Control 2) and synthetic growth media devoid of organic matter and ammonia (Control 3). (B) Open system. The SOPR of OPG biomass was determined for the first 1 h, 1-3 h period, and 3-6 period. Error bars represent the standard deviations of triplicate experiments.

Supporting Information for

The oxygenic photogranule process for aeration-free wastewater treatment

Ahmed S. Abouhend[‡§], Adam McNair[‡], Wenye C. Kuo-Dahab[‡], Christopher Watt[‡], Caitlyn S. Butler[‡], Kim Milferstedt[‖], Jérôme Hamelin[‖], Jeongmi Seo[‡†], Gitau J. Gikonyo[‡], Khalid M. El-Moselhy[§], Chul Park[‡*]

[‡]Department of Civil and Environmental Engineering, University of Massachusetts Amherst, MA 01003, USA.

[§]Marine Pollution Laboratory, National Institute of Oceanography and Fisheries, Hurghada 84511, Egypt.

[‖]LBE, Univ Montpellier, INRA, Narbonne, France.

[†]Department of Environmental Engineering, University of Seoul, Seoul, South Korea.

[*]Corresponding author: chulp@umass.edu

Detailed Materials and Methods for:

Seed photogranules. The seed photogranules were generated by hydrostatic incubation of activated sludge under a continuous source of light.[20,21] Activated sludge was collected from the aeration basin of Hadley WWTP (Hadley, MA) and 10 mL aliquots were inoculated in 20 mL glass vials. The vials were closed with plastic caps and incubated without any mixing or agitation at constant temperature (20 °C) with exposition to continuous light emitted from fluorescent bulbs. The light conditions provided a photosynthetically active radiation (PAR) of about 150 μmol/m^2-s on the top of vials. Spherical photogranules of 5-15 mm in diameter were observed in the vials after 25-35 days of hydrostatic incubation.

Imaging and particle size distribution (PSD) analysis. Images of mixed OPG biomass in Petri dishes (5 cm in diameter) were regularly collected. We used the software ImageJ[17] to determine the particle size distribution of the OPG biomass. Initially, the threshold range of biomass images was set and then biomass images were binarized. Shapes of particles were identified and their dimensions were automatically determined with a reference scale set to the Petri dish diameter. The total count of the biomass particles in the Petri dishes was also automatically quantified and used to calculate the total biomass particles in the reactor. Histograms of size-based and volume-based particle distributions were created using the Frequency Function in *MS Excel 2013.*

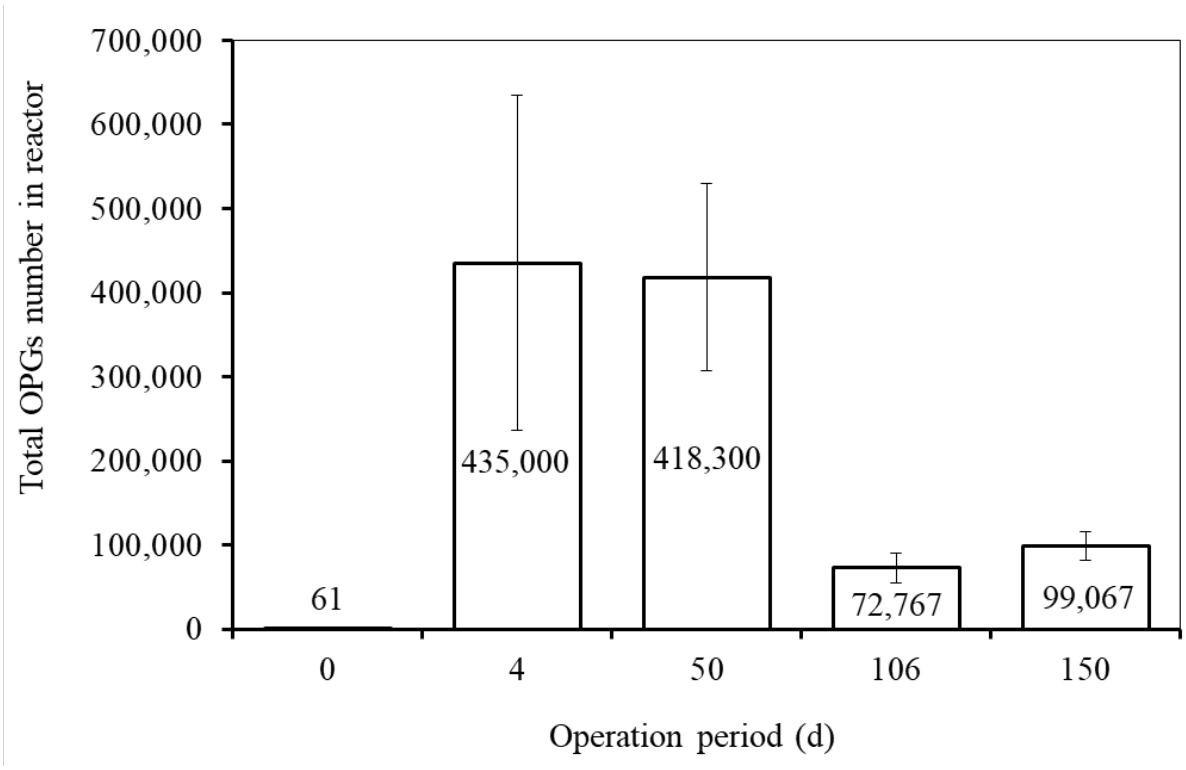

Figure S1. Changes in the total number of bioaggregates in reactors over five months of operation. Error bars represent the standard deviations of triplicate experiments.

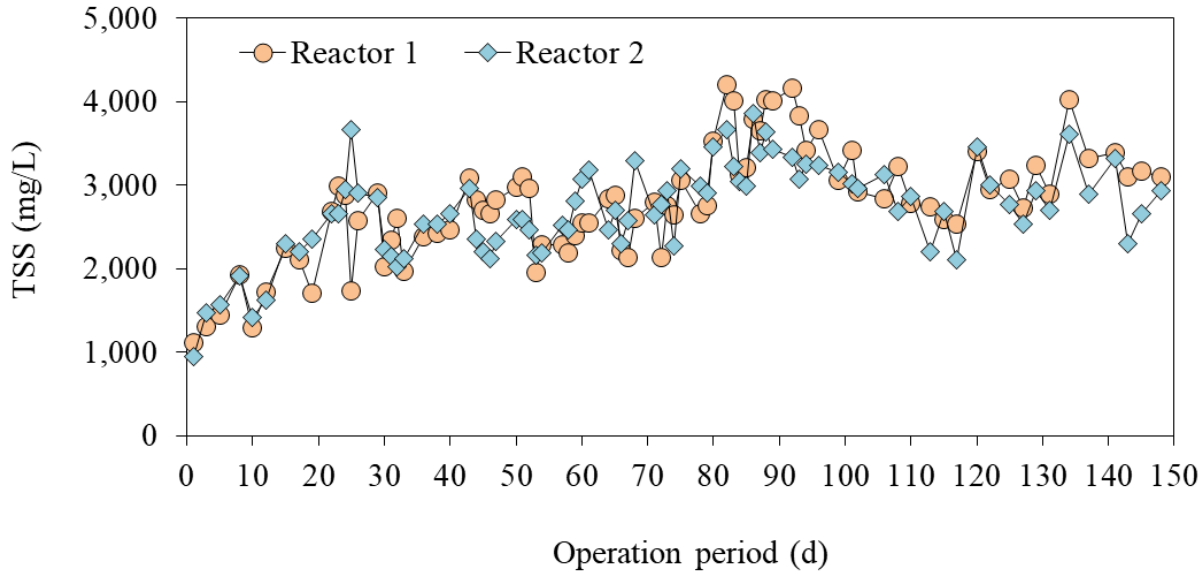

Figure S2. Dry biomass concentrations of mixed OPGs in two SBR systems.

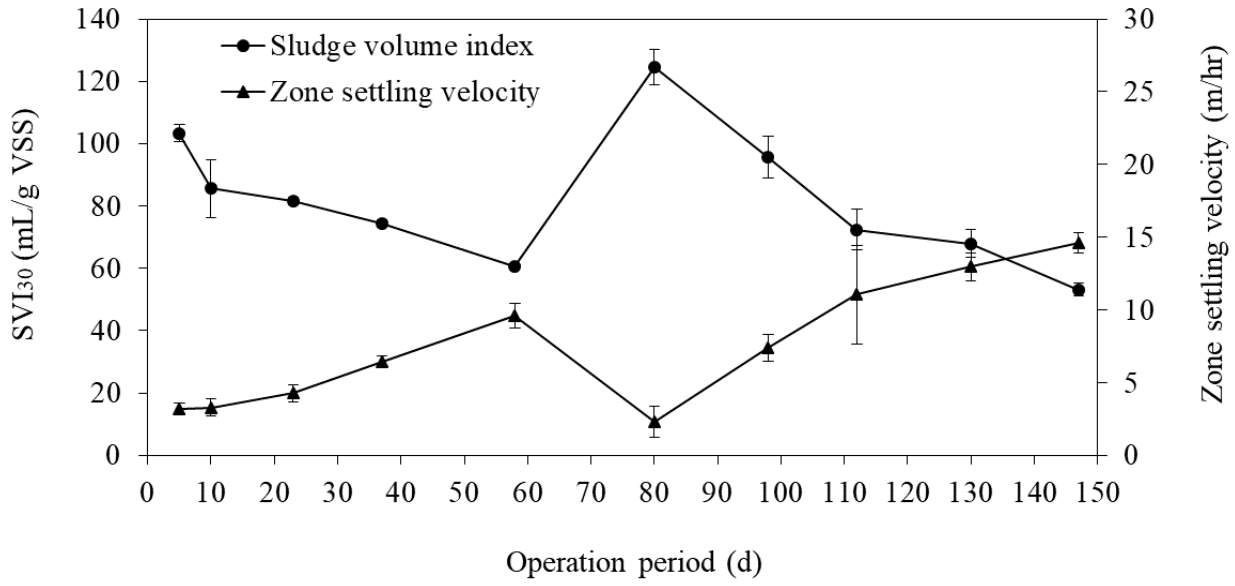

Figure S3. Changes in sludge volume index (SVI) and zone settling velocity (ZSV) of mixed OPG biomass in reactors. Error bars represent the standard deviations of triplicate experiments.

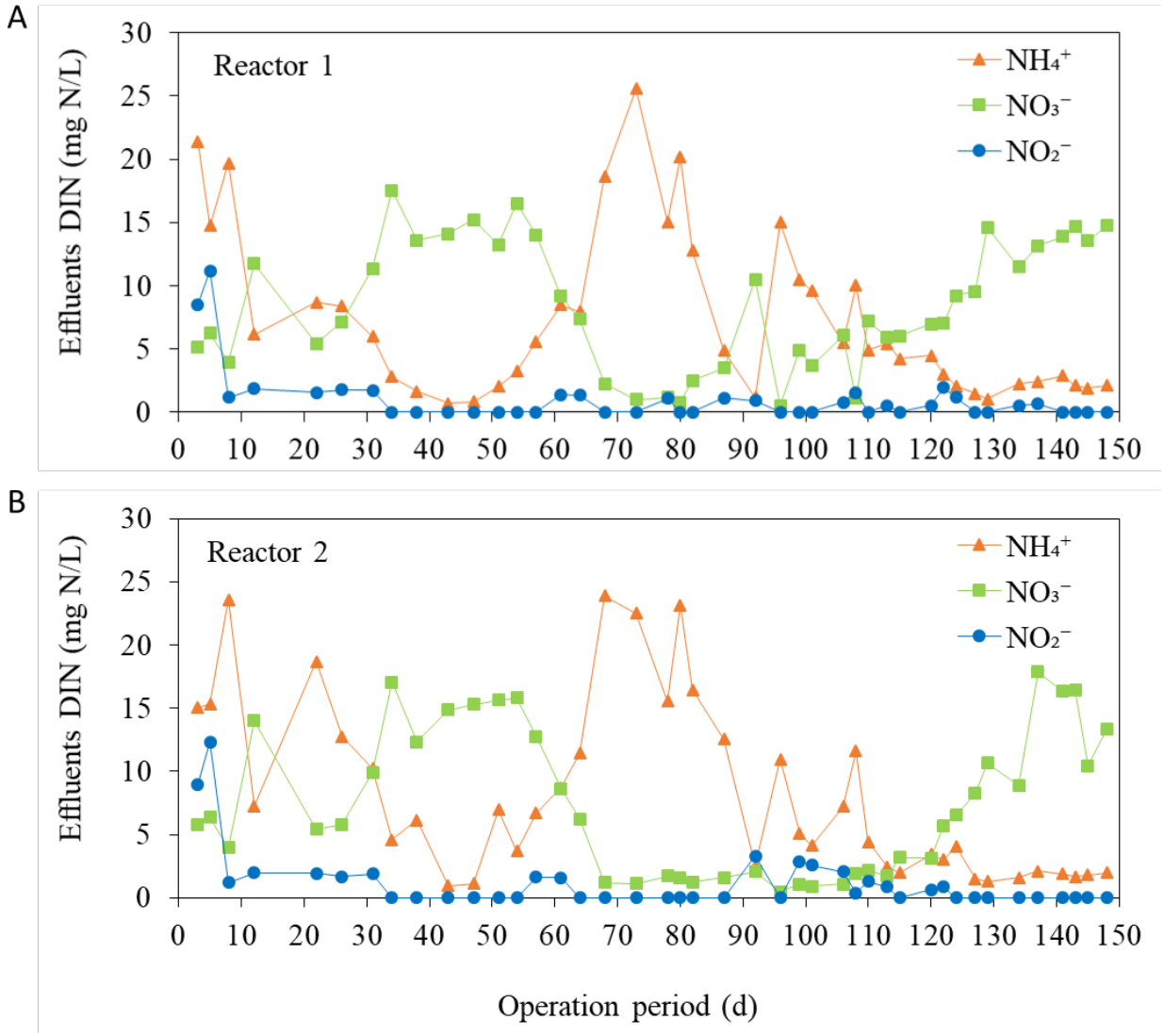

Figure S4. Profile of dissolved inorganic nitrogen (DIN) species in the effluents of SBR systems. (A) Reactor 1 DIN profile. (B) Reactor 2 DIN profile.

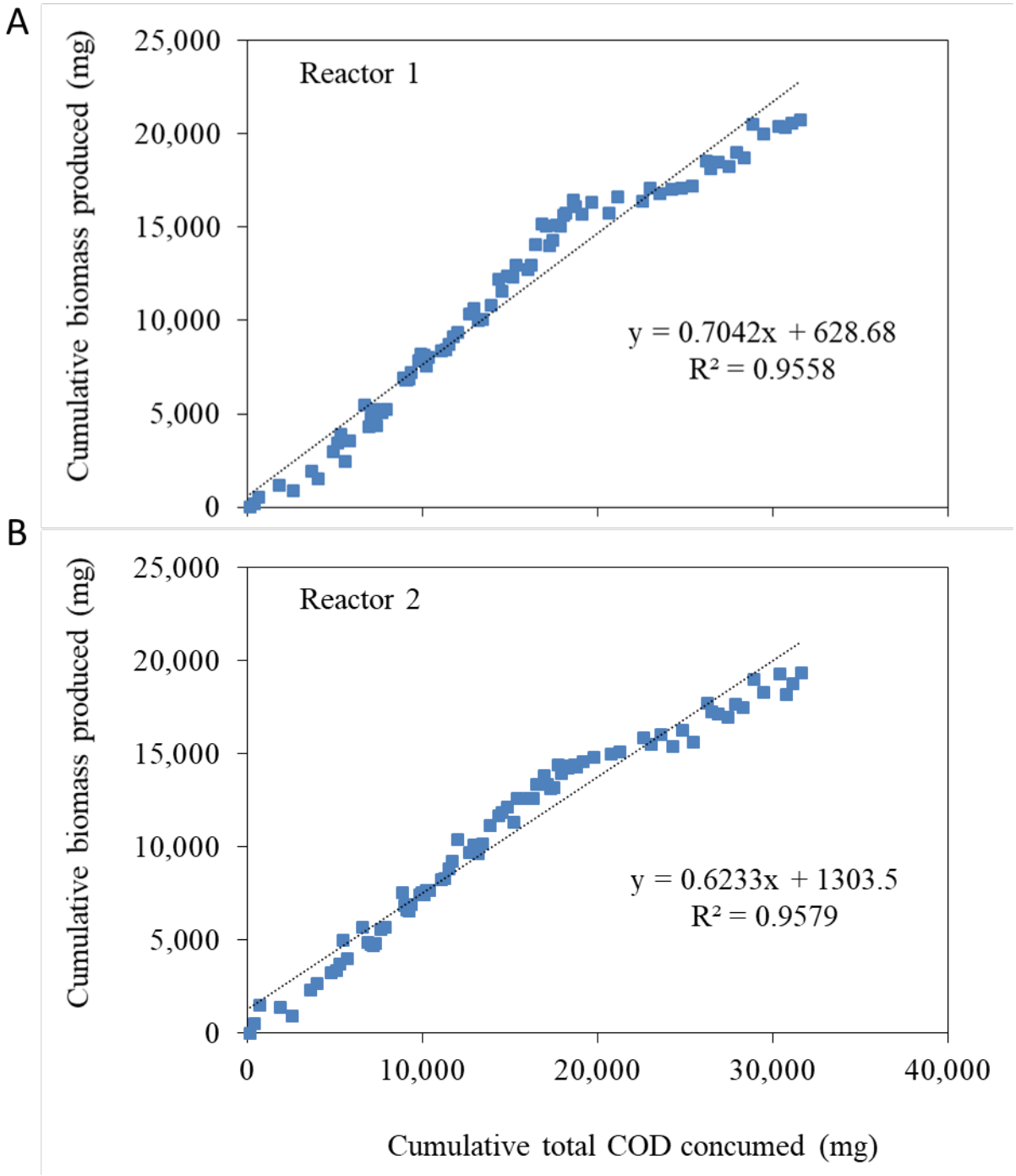

Figure S5. Linear-regression analysis on the biomass produced per total COD consumed in the OPG systems during the entire reactor operation period (150 d). (A) Reactor 1. (B) Reactor 2. The slope of each regression line indicates the observed biomass yield (mg VSS/mg tCOD). The stoichiometric ratio of COD/VSS of mixed OPG biomass was experimentally found to be1.8±0.09.